Journal of Alloys and Compounds 520 (2012) 262–265

Contents lists available at SciVerse ScienceDirect

Journal of Alloys and Compounds

journal homepage: www.elsevier.com/locate/jallcom

Judd–Ofelt analysis of spectroscopic properties of Sm^{3+} ions in K_2YF_5 crystal

Phan Van Do [a], Vu Phi Tuyen [b], Vu Xuan Quang [b], Nguyen Trong Thanh [b], Vu Thi Thai Ha [b], Nicholas M. Khaidukov [c], Yong-Ill Lee [d], B.T. Huy [d,*]

[a] Water Resources University, Hanoi, Viet Nam
[b] Institute of Materials Science, Vietnam Academy of Science and Technology, Hanoi, Viet Nam
[c] Kurnakov Institute of General and Inorganic Chemistry, Moscow, Russia
[d] Department of Chemistry, Changwon National University, Changwon 641 773, South Korea

ARTICLE INFO

Article history:
Received 13 December 2011
Received in revised form 3 January 2012
Accepted 5 January 2012
Available online 14 January 2012

Keywords:
Rare earth alloys and compounds
Crystal growth
Crystal and ligand fields
Optical spectroscopy

ABSTRACT

K_2YF_5 crystals doped Sm^{3+} ions were synthesized under hydrothermal condition. The absorption, luminescence spectra, and lifetimes of K_2YF_5:Sm^{3+} were measured at room temperature. The results were analyzed using Judd–Ofelt (JO) theory giving the values of three Ω_2, Ω_4, and Ω_6 intensity parameters. Using these JO parameters as well as from the emission, various radiative parameters such as transition probabilities (A_R), radiative lifetime (ι_R), calculated branching ratios (β_R), measured branching ratios (β_{mes}), and stimulated emission cross-sections ($\sigma_{\lambda p}$) have been calculated for $^4G_{5/2}$ excited level.

1. Introduction

Spectroscopic investigations of rare earth (RE) doped glasses provide valuable information that includes energy level structure, radiative properties, stimulated emission cross-sections, etc. These insights play a key role to improve the existing or to develop new optical devices, such as lasers, light converters, sensors, hole burning high-density memories, optical fibers, and amplifiers. K_2LnF_5 (Ln = rare earth) crystals doped with rare earth ions are important materials for optical applications such as optical amplifiers and solid-state lasers [1] and especially they are a high energy dosimeter materials of great promise [2–5]. Recently there are many reports on optical properties of the materials, such as the K_2YF_5:Nd^{3+}, K_2YF_5:Pr^{3+}, K_2YF_5:Tm^{3+}, K_2GdF_5:Tb^{3+}, and K_2GdF_5:Dy^{3+} crystals [1–3,5–7]. The authors have investigated the optical properties of these materials by using optically stimulated luminescence (OSL) [8], thermoluminescence [9], frequency upconversion fluorescence [3], site-selective laser-excitation spectroscopy [10]. It is noted that K_2YF_5 phases crystallize in orthorhombic system, each Y^{3+} ion is surrounded by seven fluoride ions forming a C_{2v} local point symmetry. The YF_7 polyhedral form chains parallel to the *c*-axis of the structure [4,7]. Samarium is one of the most popular rare earth elements, which is used extensively in optical devices; its $4f^5$ electron configuration usually exists in triply ionized (Sm^{3+}). Several authors have studied its spectra in various matrices [11–14] but to our understanding there has been no report on the optical spectra of Sm^{3+} doped in K_2YF_5 crystal.

The Judd–Ofelt (JO) theory was shown to be useful to characterize radioactive transitions for RE-doped solids, as well as aqueous solutions, and to estimate the intensities of the transitions for rare-earth ions [15–22]. This theory defines a set of three intensity parameters, Ω_λ (λ = 2, 4, 6), that are sensitive to the environment of the rare-earth ions.

In this work, we have investigated optical properties of Sm^{3+} ions-doped K_2YF_5 crystal. On the other hand, we also used the Judd–Ofelt theory to determine intensity parameters, radiative transition probabilities, branching ratios, and radiative lifetimes of $^4G_{5/2}$ excited states with analyzing the absorption spectra of K_2YF_5:Sm^{3+} crystal at room temperature. In addition, we also determined the stimulated emissions cross section for selected and briefly discussed the potential application of K_2YF_5:Sm^{3+} as efficient laser crystal.

2. Experimental

K_2YF_5 single crystals doped with 1.0 mol% of Sm^{3+} were obtained by hydrothermal synthesis at Kurnakov Institute of General and Inorganic Chemistry, Moscow, Russia. The chemical interaction of the oxide mixture $(1-x)Y_2O_3$–xSm_2O_3 with aqueous KF solutions was performed at a temperature of 750 K, a pressure of 100–150 MPa, and a temperature gradient along the reactor body of up to 3 K cm^{-1}. A proper choice of reaction conditions has allowed to obtain K_2YF_5 single crystal

* Corresponding author.
E-mail address: buithehuy.nt@gmail.com (B.T. Huy).

0925-8388/$ – see front matter.
doi:10.1016/j.jallcom.2012.01.037

[6]. The optical absorption spectra were recorded between 300 and 2000 nm using Jascco V670 spectrometer. The photoluminescence (PL) spectra were recorded by Fluorolog-3 spectrophotometer, model FL3-22, Horiba Jobin Yvon. All the measurements were carried out at room temperature.

3. Theoretical outline

3.1. Oscillator strengths and Judd–Ofelt analysis

The oscillator strengths, f_{exp}, of the absorption bands were determined experimentally using the following formula [23]:

$$f_{exp} = 4.318 \times 10^{-9} \int \alpha(\nu) d\nu \quad (1)$$

where α is molar extinction coefficient at energy ν (cm^{-1}). The $\alpha(\nu)$ values can be calculated from the absorbance A by using Lambert–Beer's law

$$A = \alpha(\nu) C d$$

where C is concentration [dim: L^{-3}, units: mol^{-1}], d is the optical path length [dim: L, units: cm].

According to the JO theory [11,23], the electric dipole oscillator strength of a transition from the ground state to an excited state is given by

$$f_{cal} = \frac{8\pi^2 mc\nu}{3h(2J+1)} \times \frac{\left(n^2+2\right)^2}{9n} \sum_{\lambda=2,4,6} \Omega_\lambda \left\langle \Psi J \left\| U^\lambda \right\| \Psi' J' \right\rangle^2 \quad (2)$$

where n is the refractive index of the material, J is the total angular momentum of the ground state, Ω_λ are the JO intensity parameters, and $\left\|U^\lambda\right\|^2$ are the squared doubly reduced matrix of the unit tensor operator of the rank $\lambda = 2, 4, 6$ are calculated from intermediate coupling approximation for a transition $\left|\psi J\right\rangle \rightarrow \left|\psi' J'\right\rangle$. The oscillator strength of the various observed transitions is evaluated through Eqs. (1) and (2). A least squares fitting approach is then used for Eq. (2) to determine Ω_λ parameters, which give the best fit between experimental and calculated oscillator strengths.

3.2. Radiative properties

The JO parameters along with refractive index, n, are used to predict the radiative properties of excited states of Ln^{3+} ion. The radiative transition probability (A_R) for $\left|\psi J\right\rangle \rightarrow \left|\psi' J'\right\rangle$ transition can be calculated from Eq. (3) [11]:

$$A_R\left(\psi J, \psi' J'\right) = \frac{64\pi^4 \nu^3}{3h(2J+1)} \left[\frac{n\left(n^2+2\right)^2}{9} S_{ed} + n^3 S_{md} \right] \quad (3)$$

The correction factors $(n^2+2)^2/9n$ in Eq. (2) and n^3 in Eq. (3) relate to the effect of the dielectric medium. The factor $(n^2+2)/9n$ represents the local field correction for the ion in the host medium. The lanthanide ion in a dielectric medium not only feels the radiation field of incident light, but also the field from the dipoles in the medium. The total field consisting of the electric field E of the incident light (electric field in the vacuum) and the electric field of the dipoles is called the effective field E_{eff}. The square of the matrix element in the electric dipole operator has to be multiplied by a factor $(E_{eff}/E)^2$. In the first approximation $(E_{eff}/E)^2 = (n^2+2)^2/9n$. This factor is the Lorentz local field correction and accounts for electric dipole correction. Similarly the correction factor for emission spectra corresponding to the magnetic dipole transition is n^3.

$$S_{ed} = e^2 \sum_{\lambda=2,4,6} \Omega_\lambda \left| \left\langle \Psi J \left\| U^\lambda \right\| \Psi' J' \right\rangle \right|^2 \quad (4)$$

Table 1
Energy transitions (E), bonding parameters (δ), the experimental (f_{exp}) and calculated (f_{cal}) oscillator strengths for K_2YF_5:Sm^{3+} crystal.

Transition $^6H_{5/2} \rightarrow$	E_{exp} (cm^{-1})	E_{aquo} (cm^{-1})	f_{exp} ($\times 10^{-6}$)	f_{cal} ($\times 10^{-6}$)
$H_{15/2}$	6514	6508	0.46	0.02
$^6F_{3/2}$	6761	6641	1.00	0.96
$^6F_{5/2}$	7358	7100	1.13	1.78
$^6F_{7/2}$	8149	8100	2.03	2.77
$^6F_{9/2}$	9276	9200	2.70	1.79
$^6F_{11/2}$	9990	10,050	1.03	0.27
$^4I_{11/2}$	21,052	21,100	1.22	0.12
$^4I_{13/2}$	21,413	21,600	1.05	0.44
$^4I_{15/2}$	22,950	22,966	2.21	0.23
$^6P_{5/2}$	23,923	24,050	2.59	0.53
$^6P_{3/2}$	24,938	24,950	4.60	3.63
	$\bar{\beta} = 1.0053$,	$\delta = -0.53$	rms = 1.33×10^{-6}	

$$S_{md} = (e^2h^2/16\pi^2m^2c^2)\left|\left\langle \Psi J \left| L + 2S \right| \Psi' J' \right\rangle\right|^2 \quad (5)$$

where S_{ed} and S_{md} are the electric and magnetic dipole line strengths, the S_{md} values do not depend on the host material. The total radiative transition probability (A_T), the radiative lifetime (τ_R), and branching ratio (β_R) of an excited state are given by

$$A_T(\psi, J) = \sum_{\psi' J'} A(\psi J, \psi' J') \quad (6)$$

$$\tau_R(\psi J) = \left[A_T(\psi J)\right]^{-1} \quad (7)$$

$$\beta_R(\psi J \rightarrow \psi' J') = \frac{A(\psi J \rightarrow \psi' J')}{A_T(\psi J)} \quad (8)$$

The branching ratio can be used to predict the relative intensities of all emission lines originating from a given excited state. The experimental branching ratios can be found from the relative areas of the emission bands. The stimulated emission cross section $\sigma(\lambda_P)$ is related to the radiative transition probability (A) and can be expressed as

$$\sigma(\lambda_P) = \left(\frac{\lambda_P^4}{8\pi c n^2 \Delta\lambda_{eff}} \right) A(\psi J, \psi' J') \quad (9)$$

where λ_P is the transition peak wavelength and $\Delta\lambda_{eff}$ is its effective linewidth found by dividing the area of the emission band by its average height.

4. Results and discussion

4.1. Absorption spectrum

The absorption spectra of K_2YF_5 crystal doped with 1.0 mol% of Sm^{3+} ions are shown in Fig. 1a for the regions 380–500 nm and Fig. 1b for the regions 900–1600 nm. All the absorption bands originate from the ground state, $^6H_{5/2}$. The band positions along with assignments for K_2YF_5:Sm^{3+}crystal are shown in Table 1, which are also compared with Sm^{3+}-diluted acid solution (aqua-ion) system [24].

4.2. Nephelauxetic effect – Bonding parameter

The bonding parameter (δ) is defined as $\delta = \left[\left(1 - \bar{\beta}\right)/\bar{\beta}\right] \times 100$ [10], where $\bar{\beta} = (\sum \beta)/n$ and β (nephelauxetic ratio) = ν_c/ν_a, ν_c and ν_a are energies of the corresponding transitions in the complex and aqua-ion [11], respectively, and n refers to the number of levels that are used to compute $\bar{\beta}$ values. The bonding parameter depends on the environmental field; δ can be received the positive or negative value indicating covalent or ionic bonding. In our sample, the values of β and δ bonding parameter are 1.0053, −0.53, respectively. Thus,

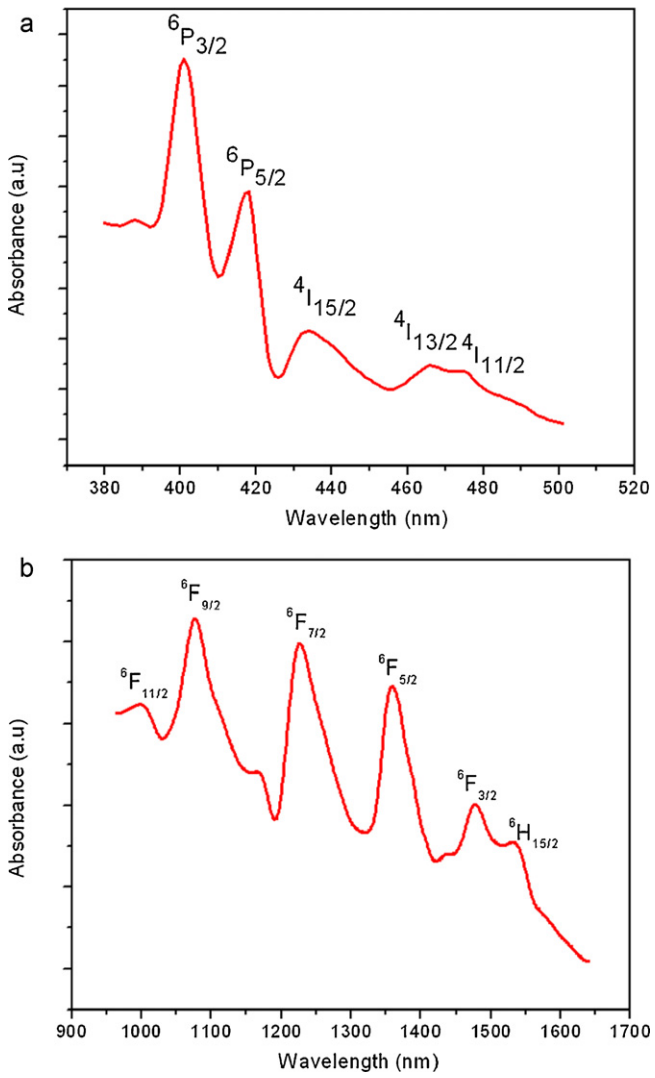

Fig. 1. The absorption spectrum of K_2YF_5:Sm^{3+} crystal in range 380–500 nm (a) and 900–1600 nm (b).

in this case the bonding of Sm^{3+} ions with the local host is ionic bonding.

4.3. Oscillator strengths, JO parameters

From the absorption spectra of the K_2YF_5:Sm^{3+} crystal, the experimental (f_{exp}) and calculated (f_{cal}) oscillator strengths were determined using Eqs. (1) and (2) and the results are presented in Table 1. The JO parameters have been calculated by using the oscillator strengths of observed absorption bands and doubly reduced matrix elements by least square fit approximation. These reduced matrix elements did not depend on host matrix as noticed from earlier studies [24,25].

Table 2 displays the Ω values of our sample in comparison with different matrix [11–14]. The Ω_2 value of our crystal is smaller than that of the different hosts. The characteristic feature of the Ω_2 is that it is sensitive to the local environment of the RE ions and is often related with the asymmetry of the coordination structure, polarizability of ligand ions or molecules, and bonding nature [26]. The Ω_2 parameter in K_2YF_5:Sm^{3+} crystal is smaller than that of other hosts that can be attributed to higher symmetry of the coordination structure surrounding the RE ion. In addition, the presence of the F^{-1} ions plays the important role for the reduction of Ω_2 value. It is well known, the fluorine ions have the highest

Table 2
The JO parameters for Sm^{3+} doped various hosts.

Host matrix	Ω_2 ($\times10^{-20}$ cm^2)	Ω_4 ($\times10^{-20}$ cm^2)	Ω_6 ($\times10^{-20}$ cm^2)	Refs.
K_2YF_5	0.38	3.55	2.18	Present
59.50 Li_2CO_3–39.5 H_2BO_3	6.99	12.00	8.47	[11]
Li_2O–BaO–La_2O_3–B_2O_3	6.81	4.43	2.58	[12]
49.50 Li_2CO_3–49.5 H_2BO_3	6.21	9.68	7.16	[11]
39.50 Li_2CO_3–59.5 H_2BO_3	4.71	10.33	6.50	[11]
H_2BO_3–LiF	2.34	7.54	5.40	[11]
P_2O_5–K_2O–KF–BaO–Al_2O_3	1.50	3.75	1.89	[14]
PbO–PbF_2	1.16	2.60	1.40	[13]

electronegativity (~4) in comparison with the other anion ions, therefore the RE-F bonds have the smaller covalency bond than other RE-anion bonds. This is the main reason for the reduction of the Ω_2 values in the fluoride compounds.

4.4. Fluorescence properties

Fig. 2 displays the emission spectra of K_2YF_5:Sm^{3+} crystal at excitation wavelength of 385 nm of Xenon lamp source. It exhibits four emission bands at 561, 597, 640, and 705 nm which are assigned to $^4G_{5/2} \rightarrow {}^6H_{5/2}$, $^6H_{7/2}$, $^6H_{9/2}$, and $^6H_{11/2}$ transitions, respectively. The radiative transition rates (A_R), radiative lifetime (τ_R), stimulated emission cross section $\sigma(\lambda_P)$, branching ratios (β_R), and measured ratios (β_{mes}) were determined for the $^4G_{5/2}$ by using Eq. (3), (7), (9), and (8), as displayed in Table 3.

From the values of radiative transition probabilities in Table 3, it is noted that $^4G_{5/2} \rightarrow {}^6H_{7/2}$ transition has the highest radiative transition rate in comparison with the other transitions. Hence this transition is very useful for laser emission. In general, the luminescence branching ratio is a critical parameter to the laser designer, because it characterizes the possibility of attaining stimulated emission from any specific transition. In this work, the predicted branching ratio of $^4G_{5/2} \rightarrow {}^6H_{7/2}$ transition gets a maximum value and be 50.6% whereas the measured ratio is 56.5%. Thus

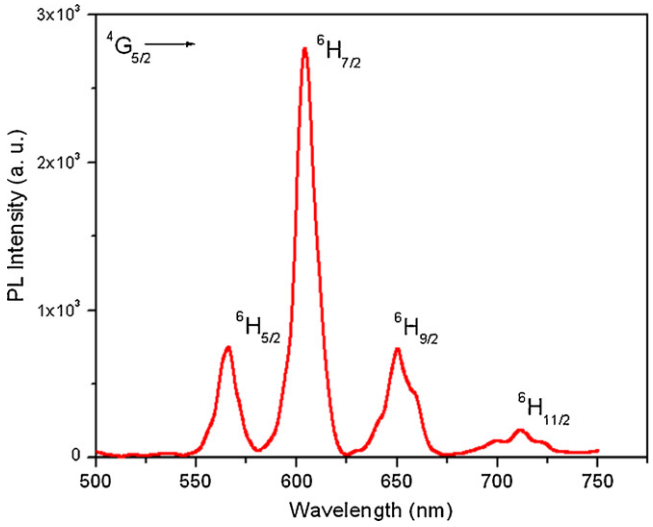

Fig. 2. The emission spectrum of Sm^{3+}:K_2YF_5 crystal.

Table 3
Predict the radiative transition rates, branching ratios and radiative lifetime of $^4G_{5/2}$ level.

Transition $^4G_{5/2}\rightarrow$	E (cm^{-1})	A_R	β_R (%)	β_{mes} (%)	$\sigma(\lambda_P)$ (10^{-22} cm^2)	τ_R (ms)
$^6F_{11/2}$	6851	0.20	0.10	–	–	5.18
$^6F_{9/2}$	8350	0.54	0.27	–	–	
$^6F_{172}$	9637	2.45	1.27	–	–	
$^6F_{5/2}$	10,493	4.43	2.30	–	–	
$^6F_{3/2}$	11,016	0.43	0.22	–	–	
$^6H_{15/2}$	11,091	0.25	0.13	–	–	
$^6F_{1/2}$	11,203	0.22	0.11	–	–	
$^6H_{13/2}$	12,578	3.87	2.01	–	–	
$^6H_{11/2}$	14,025	27.30	14.10	6.71	0.19	
$^6H_{9/2}$	15,480	50.50	26.20	18.39	0.41	
$^6H_{7/2}$	16,667	97.60	50.60	56.48	0.64	
$^6H_{5/2}$	17,762	5.31	2.75	18.42	0.03	

there is a good agreement between experimental and calculated branching ratios.

Further, the large value of branching ratio suggests that this transition can give rise to lasing action. The stimulated emission cross-section $\sigma(\lambda_P)$ is an important parameter and its value signifies rate of energy extraction from the lasing material. The values of $\sigma(\lambda_P)$ for $^4G_{5/2}$ emission transition are in the order of $^4G_{5/2} \rightarrow {}^6H_{7/2} > {}^6H_{9/2} > {}^6H_{5/2} > {}^6H_{11/2}$. It is found that $^4G_{5/2} \rightarrow {}^6H_{7/2}$ transition exhibits maximum $\sigma(\lambda_P)$ (0.64×10^{-22} cm^2), these results are in agreement with previous reports [12–14]. The measured and calculated lifetimes of $^4G_{5/2}$ level are 4.85 ms and 5.18 ms, respectively. The discrepancy between the measured and calculated lifetimes may be due to the additional non-radiative and energy transfer through cross-relaxation.

5. Conclusions

The present study yields a detailed picture of the spectral characteristics of Sm^{3+} ions in K_2YF_5 crystal. The experimental and calculated oscillator strengths of absorption transitions of K_2YF_5:Sm^{3+} were determined. By using JO theory, we determined the intensity parameters (Ω_λ) and predicted radiative lifetime (ι_R), branching ratios (β_R). These predicted values are in good agreement with experimental values. The negative value of bonding parameter δ and the small value of intensity parameter Ω_2 show that the bonding of Sm^{3+} ions with the local host is ionic bonding and the coordination structure surrounding the RE ion has high symmetry.

Acknowledgment

The authors gratefully acknowledge support for this research from Vietnam's National Foundation and for Science and Technology Development (NAFOSTED) with project code 103.06-2011.58.

References

[1] D. Wang, Y. Guo, Q. Wang, Z. Chang, J. Liu, J. Luo, J. Alloys Compd. 474 (2009) 23–25.
[2] N. Kristianpoller, D. Weiss, N. Khaidukov, V. Makhov, R. Chen, Radiat. Meas. 43 (2007) 245–248.
[3] D. Wang, Y. Min, S. Xia, V.N. Makhov, N.M. Khaidukov, J.C. Krupa, J. Alloys Compd. 361 (2003) 294–298.
[4] E.C. Silva, N.M. Khaidukov, M.S. Nogueira, L.O. Faria, Radiat. Meas. 42 (2007) 311–315.
[5] H.K. Hanh, N.M. Khaidukov, V.N. Makhov, V.X. Quang, N.T. Thanh, V.P. Tuyen, Nucl. Instrum. Methods Phys. Res. B 268 (2010) 3344–3350.
[6] M. Yin, Y. Li, N. Dong, V.N. Makhov, N.M. Khaidukov, J.C. Krupa, J. Alloys Compd. 353 (2003) 95–101.
[7] M.A. Dubinskii, N.M. Khaidukov, I.G. Garipov, L.N. Dem'Yanets, A.K. Naumov, V.V. Semashko, V.A. Malyusov, J. Mod. Opt. 37 (1990) 1355–1360.
[8] J. Marcazzó, E. Cruz-Zaragoza, V. Xuan Quang, N.M. Khaidukov, M. Santiago, J. Lumin. 131 (2011) 2711–2715.
[9] J. Marcazzo, M. Santiago, E. Caselli, N. Nariyama, N.M. Khaidukov, Opt. Mater. 26 (2004) 65–70.
[10] K.H. Jang, E.S. Kim, L. Shi, N.M. Khaidukov, H.J. Seo, Opt. Mater. 31 (2009) 1819–1821.
[11] C.K. Jayasankar, P. Babu, J. Alloys Compd. 307 (2000) 82–95.
[12] H. Lin, D. Yang, G. Liu, T. Ma, B. Zhai, Q. An, J. Yu, X. Wang, X. Liu, E. Yue-Bun Pun, J. Lumin. 113 (2005) 121–128.
[13] P. Nachimuthu, R. Jagannathan, V. Nirmal Kumar, D. Narayana Rao, J. Non-Cryst. Solids 217 (1997) 215–223.
[14] T. Suhasini, J. Suresh Kumar, T. Sasikala, K. Jang, H.S. Lee, M. Jayasimhadri, J.H. Jeong, S.S. Yi, L. Rama Moorthy, Opt. Mater. 31 (2009) 1167–1172.
[15] P.A. Azeem, S. Balaji, R.R. Reddy, Spectrochim. Acta A 69 (2008) 183–188.
[16] Q. Su, H. Liang, C. Li, H. He, Y. Lu, J. Li, Y. Tao, J. Lumin. 122–123 (2007) 927–930.
[17] K.S.V. Sudhakar, M. Srinivasa Reddy, L. Srinivasa Rao, N. Veeraiah, J. Lumin. 128 (2008) 1791–1798.
[18] B.T. Huy, Min-Ho Seo, Jae-Min Lim, Yong-Ill Lee, N.T. Thanh, V.X. Quang, T.T. Hoai, N.A. Hong, J. Korean Phys. Soc. 59 (2011) 3300–3307.
[19] A. Agarwal, I. Pal, S. Sanghi, M.P. Aggarwal, Opt. Mater. 32 (2009) 339–344.
[20] H. Ahrens, M. Wollenhaupt, P. Fröbel, J. Lin, K. Bärner, G.S. Sun, R. Braunstein, J. Lumin. 82 (1999) 177–186.
[21] P. Němec, J. Jedelský, M. Frumar, J. Non-Cryst. Solids 326–327 (2003) 325–329.
[22] V. Venkatramu, P. Babu, C.K. Jayasankar, T. Tröster, W. Sievers, G. Wortmann, Opt. Mater. 29 (2007) 1429–1439.
[23] G.S. Ofelt, J. Chem. Phys. 37 (1962) 511–520.
[24] W.T. Carnall, P.R. Fields, K. Rajnak, J. Chem. Phys. 49 (1968) 4424–4442.
[25] W.T. Carnall, P.R. Fields, B.G. Wybourne, J. Chem. Phys. 42 (1965) 3797–3806.
[26] R. Praveena, R. Vijaya, C.K. Jayasankar, Spectrochim. Acta A 70 (2008) 577–586.